EVALUATION OF MECHANICAL STRESSES IN STRUCTURAL STEELS BY THE DISTRIBUTION OF CRITICAL MAGNETIC FIELDS

E. S. GORKUNOV[1], S. M. ZADVORKIN[1], E. I. YAKUSHENKO[2], A. N. MUSHNIKOV[1]
[1] INSTITUTE OF ENGINEERING SCIENCE, RAS (Ural Branch), Ekaterinburg, Russia
[2]NAVAL ENGINEERING INSTITUTE, St. Petersburg, Russia

The application of magnetic methods is a promising trend in estimating the stress-strain state of structural components. A number of works discussed the effect of elastic and plastic deformations on magnetic parameters [1–6]. It is coercive force that is most often used as a test parameter. Particularly, the strain dependences of coercive force in low- and mid-carbon and low-alloy steels under tension were shown to be qualitatively similar to the stress-strain diagram [5, 6]. However, the practically important region of elastic strain, due to the effect of induced magnetic anisotropy, display nonmonotonic strain dependences of the coercive force and other characteristics of a hysteresis loop and the magnetization curve. Therefore it seems topical to develop nondestructive methods for evaluating strains and stresses in ferromagnetic structural materials with invoking physical phenomena enabling one to obtain a unique relationship of magnetic characteristics to the parameters of the stress-strain state. It is shown in [7] that it is promising to study the distribution of critical magnetic fields during magnetization and magnetization reversal for purposes of magnetic structuroscopy of thermally treated steels. As compared to measuring the coercive force, which represents the integral properties of a ferromagnet, studies of the kind offer more accurate information on the behaviour of the processes of magnetization and magnetization reversal, on the interaction of domain walls with certain types of defects. Besides, investigations into the distribution of critical magnetic fields enable one to obtain information on the volume of a ferromagnet that has changed its state in a magnetic field of specified strength at certain mechanical stresses, and thus to predict the level of change in magnetic moment and possible radiation of electromagnetic waves under deformation.

The research was done on specimens made of structural steel 15CrNi4Cu (see the chemical composition in the table).

Table. The chemical composition of the steel under study.

Element	C	Si	Mn	Cr	Ni	Cu
Content, %	0.15	0.13	0.34	0.69	4.11	1.23

Magnetic measurements under uniaxial compression were made at stresses ranging between 0 and −192 MPa in tension testing to the onset of the developed plastic strain stage (the conventional yield stress of the steel is 900 MPA), and in torsion testing to fracture.

The amount of strain on the i-th step of tensile or compressive deformation was determined by the formula

$$\varepsilon_i = ln(l_i/l_0), \quad (1)$$

where l_0 is calculated initial specimen length; l_i is calculated specimen length after the i-th loading.

On the i-th step of tensile stress σ_i was determined by the formula

$$\sigma_i = P_i/S_i, \quad (2)$$

where P_i is the load applied to the specimen on the i-th step of loading, S_i is specimen cross section area at the i-th step of loading, which was found from the volume constancy condition for the gauge part of the specimen.

The average amount of torsional strain over the cross section of the specimen gauge part was determined by the formula

$$\varepsilon_{iav} = \frac{2}{3} \times \frac{\varphi_i \cdot D}{2 \cdot l_0 \cdot \sqrt{3}}, \quad (3)$$

where φ_i is current torsion angle, rad; D is gauge part diameter.

Torsional stress was determined by the formula

$$\tau_i = T_i \cdot \frac{16}{\pi D^3}, \quad (4)$$

where T_i is current torque.

Magnetic measurements were made in a closed magnetic permeameter-type circuit. A magnetic field was applied along the tension axis, the induction search coil axis being also parallel to the tension axis. The intensity of the internal magnetic field H was measured by an arch-shaped magnetic potentialmeter, and magnetic induction B was measured by a passage coil with the compensated air gap effect. The coercive force H_c and remanent induction B_r were determined by the major hysteresis loops, and the values of the coercive force $h_c^{0.4}$ and $h_c^{0.05}$ were determined by minor hysteresis loops at the maximum magnetic induction of 0.4 and 0.05 T respectively. Besides, the maximum magnetic permeability μ_{max} was determined by the normal magnetization curve.

In order to study the distribution of critical fields in the bulk of a ferromagnet in magnetization from the statically demagnetized state and magnetization reversal from the remanent state after magnetization in the field of 600 A/cm, the values of remanent inductions obtained from the magnetization curve $B_r(H)$ (Fig.1a) and the descending hysteresis branch $B^-_d(H)$ were determined (Fig.1b). The curves obtained by differentiating $B_r(H)$ and $B^-_d(H)$ with respect to H are critical field distribution spectra, which are sometimes referred to as magnetic rigidity spectra [8] for a given ferromagnet. These spectra characterize irreversible changes occurring in a ferromagnet under magnetization (primary spectrum) and magnetization reversal (secondary spectrum). The primary rigidity spectrum is the distribution of critical fields H_{cr} during specimen magnetization, and it characterizes the irreversible changes of magnetization in the relative volume equal to $\frac{\Delta \hat{A}_r}{\Delta \acute{I} \cdot \hat{A}_{r\max}} \cdot \acute{I}_{cr}$. The secondary spectrum is similar to the primary one, but it represents the irreversible changes of magnetization during magnetization reversal in the volume $\frac{\Delta \hat{A}^-_d}{2\Delta \acute{I} \cdot \hat{A}_{r\max}} \cdot \acute{I}_{cr}$.

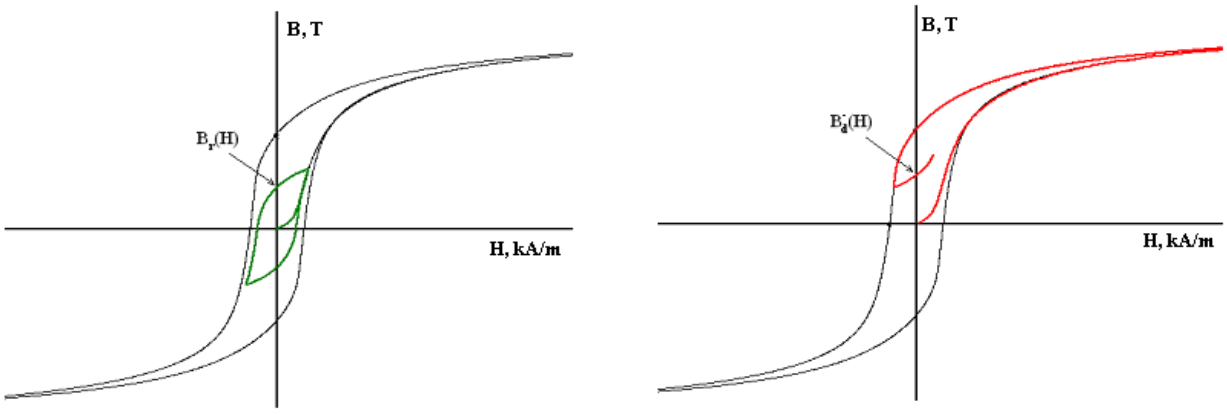

a *b*

Fig. 1. Determination of remanent induction obtained from the magnetization curve (*a*) and the descending branch of magnetic hysteresis (*b*).

The values of the coercive force, remanent induction and maximum magnetic permeability, all found from the major hysteresis loop, as dependent on tensile and compressive stresses σ are shown in Fig. 2. These dependences can be represented as resulting from the formation of the magnetic texture of stresses [1]: elastic compressive stresses cause an increase in the coercive force and a decrease in remanent induction and maximum magnetic permeability (negative magnetoelastic effect, $\sigma\lambda_s < 0$, where λ_s is saturation magnetostriction); tensile stresses decrease H_c and increases B_r and μ_{max} (positive magnetoelastic effect, $\sigma\lambda_s > 0$).

Figure 2 depicts σ-dependences of $h_c^{0.4}$ and $h_c^{0.05}$ found from minor cycles of magnetization reversal of steel 15CrNi4Cu in medium and weak fields. Note that the coercive force $h_c^{0.05}$ measured by minor magnetic hysteresis cycles in weak fields (the Rayleigh region) grows monotonically with normal elastic stresses, whereas H_c and $h_c^{0.4}$ decrease as σ grows. As the mobility of 180° domain walls is much higher than that of 90° ones, the critical field values of the former being lower [1], magnetization reversal and, accordingly, magnetic hysteresis in weak fields are predominantly associated most likely with the displacement of 180° domain boundaries. Therefore the magnetoelastic effect occurring in the magnetization of steel 15CrNi4Cu to the maximum magnetic induction of 0.05 T manifests itself rather insignificantly.

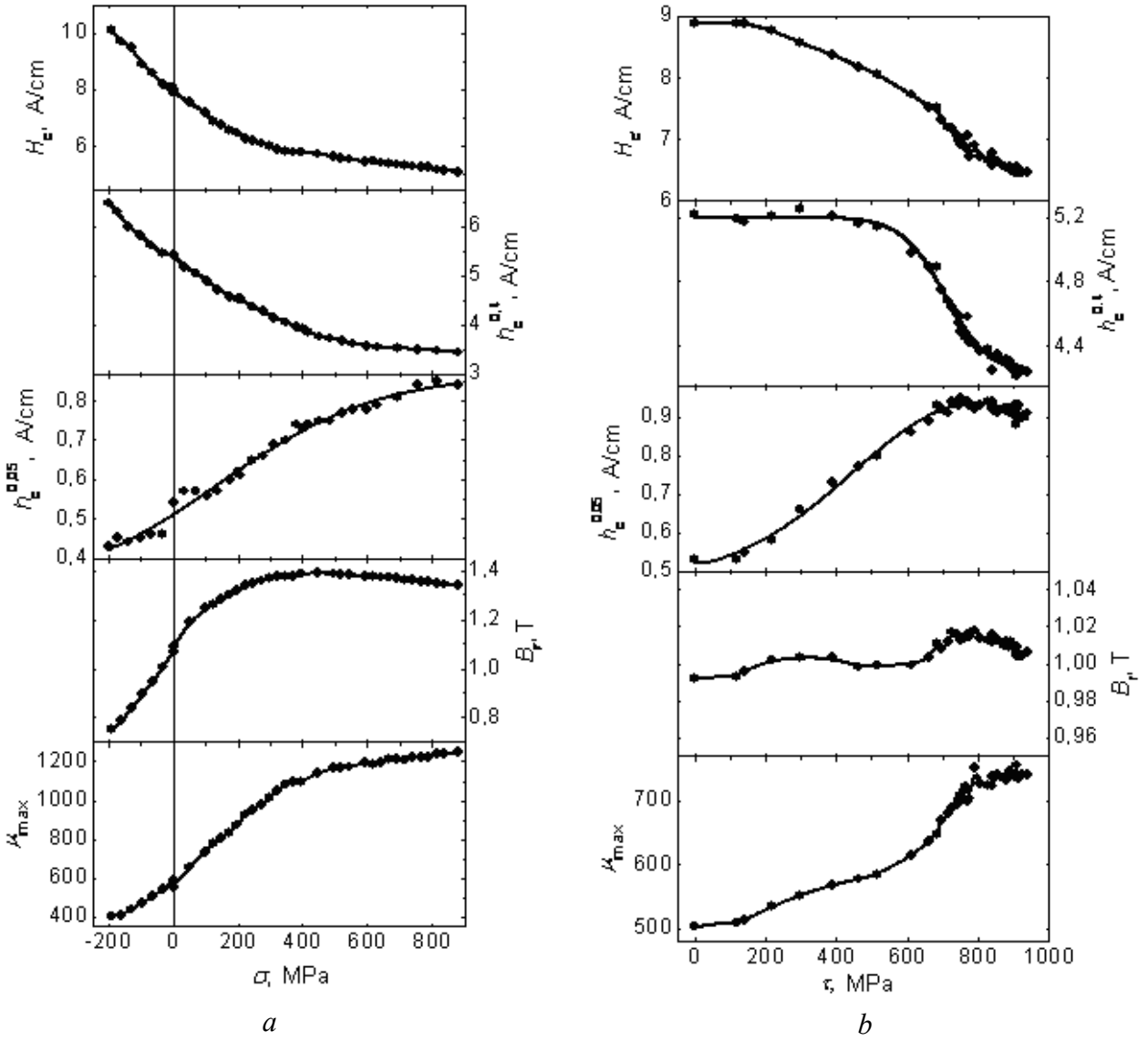

Fig. 2. Magnetic characteristics of steel 15CrNi4Cu as dependent on normal (*a*) and tangential (*b*) stresses.

Figure 2 also shows magnetic characteristics of the steel under shearing stresses τ in torsion. As τ grows, the coercive force on the major magnetic hysteresis loop and on the minor cycle of magnetization reversal with maximum induction of 0.4 T decreases, and the maximum magnetic permeability increases. Remanent induction tends to rise with τ, however, the changes of B_r do not exceed 2%, and this is within the measurement error range. The same way as under uniaxial tension/compression, $h_c^{0,05}$ grows monotonically with mechanical stresses under shearing strain.

Thus, it is obvious from Fig. 2 that the magnetic characteristics that have been studied, except

remanent induction, vary uniquely with stresses, and, in principle, they can be used as parameters in magnetic testing of elastic strains and stresses in structural members.

Figures 3a, 4a, 5a and 3b, 4b, 5b show, respectively, the primary and secondary spectra of the magnetic rigidity of the specimens. The peaks of the field dependences of $\frac{\Delta B_r}{\Delta H \cdot B_{r\max}}$ and $\frac{\Delta B_d^-}{2\Delta H \cdot B_{r\max}}$ at different stresses a little exceed the values of the coercive force of the specimens. The peaks of the secondary spectra are narrower than those of the primary ones, i. e., the essential processes in magnetization reversal from the remanence state after magnetization in the field of 600 A/cm follow a little easier that in magnetization from the statically demagnetized state. As the compressive stress grows, the peaks of the magnetic rigidity spectra shift into the region of stronger fields, they become lower and wider. As the tensile or torsional stresses grow, the spectrum peaks shift into the region of weaker fields, they become higher and narrower.

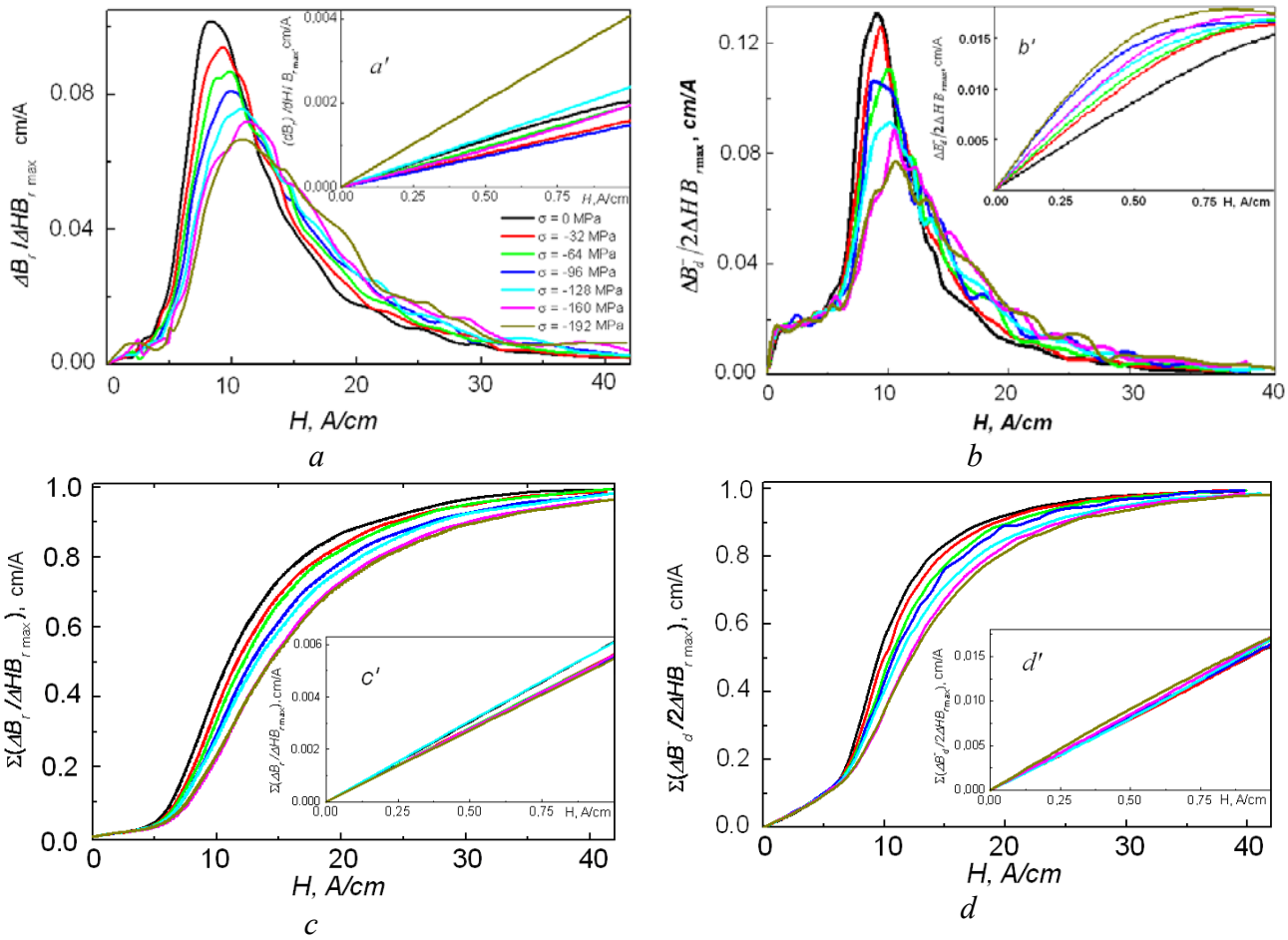

Fig. 3. The primary (*a*) and secondary (*b*) spectra of magnetic rigidity and the distributions of volume fractions of critical fields under magnetization (*c*) and magnetization reversal (*d*) in compression testing of steel 15CrNi4Cu. The initial portions of the rigidity spectra (*a', b'*) and the distributions of the critical field volumes (*c', d'*).

Figures 3c, 4c, 5c and 3d, 4d, 5d show the distribution of the volume fractions of the critical fields of the rigidity spectra $\Sigma(\Delta B_r / \Delta HB_{rmax})$ and $\Sigma(\Delta B^-_d / 2\Delta HB_{rmax})$. These volume fractions are proportional to the ferromagnet volume that has undergone magnetization (in the instances of primary spectra) or magnetization reversal (in the instances of secondary spectra) under an applied magnetic field of strength *H*. Thus, according to Fig. 3c, in the fields corresponding to the values of the coercive force it is about one-third of the volume of the compressed specimen that becomes

magnetized. In the field of 30 A/cm 90 to 95 % of the specimen volume is magnetized, depending on the stress. Magnetisation reversal proceeds a little easier than magnetization and, as follows from Fig. 3d, in the fields corresponding to the coercive force values about half of the specimen volume becomes magnetized. Also note that the higher the compressive stress, the smaller specimen volume is magnetized (reverse-magnetized) in the field of strength *H*.

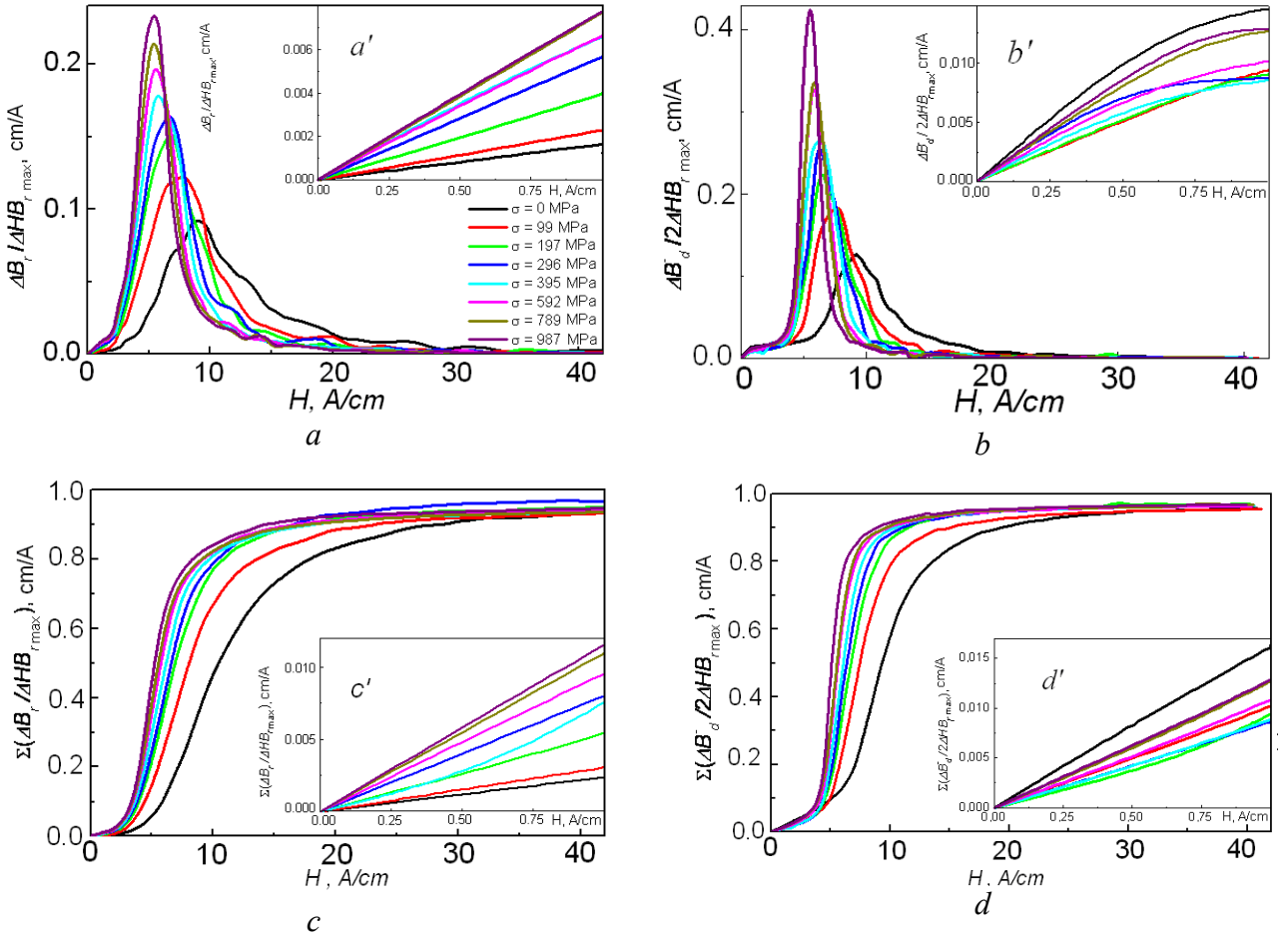

Fig. 4. The primary (*a*) and secondary (*b*) spectra of magnetic rigidity and the distributions of the volume fractions of critical fields under magnetization (*c*) and magnetization reversal (*d*) in tension testing of steel 15CrNi4Cu. The initial portions of the rigidity spectra (*a', b'*) and the distributions of the critical field volumes (*c', d'*).

Tensile stresses have an opposite effect, namely, as the stress increases, the volume of the specimen magnetized (reverse-magnetized) in the field of a given strength grows. According to Fig. 4c, at stresses higher than 200 MPa in fields corresponding to the coercive force values more than 80% of the specimen is magnetized. Figure 4d demonstrated that magnetisation reversal proceeds easier than magnetization, as it does in compression tests.

The behaviour of the magnetic rigidity spectra and the distributions of the volume fractions of the critical magnetic fields in torsion tests (Fig. 5) is similar to that under tension. The magnetized (reverse-magnetized) specimen volume in a field of given strength grows with the torsional stress. Note that, when the torsion angle increases 3 times (from 10° to 30°), tangential stresses grow approximately by 15 % (from 611 to 716 MPa), and the magnetic rigidity spectra change only slightly (Fig.5a). Thus, The form of the magnetic rigidity spectra are predominantly affected by stresses rather than by strains.

The insets in Figs. 3a, 4a, 5a and 3b, 4b, 5b show the initial areas (Rayleigh region) of magnetic rigidity spectra for the steel under study. Under the effect of compressive stress, the curves

representing the field dependences of the quantities $\frac{\Delta B_r}{\Delta H \cdot B_{r\max}}$ (primary spectra) and $\frac{\Delta \hat{A}_d^-}{2\Delta \acute{I} \cdot \hat{A}_{r\max}}$ (secondary spectra) are seen to lie a little higher than at $\sigma = 0$. At the same time, as stated above, as compressive stress grows, the magnetic rigidity spectrum peaks shift into the region of stronger fields and become lower. Thus, compressive stresses have a negative effect on the portions of the primary and secondary spectra of magnetic rigidity in weak fields and near the peaks of the spectra.

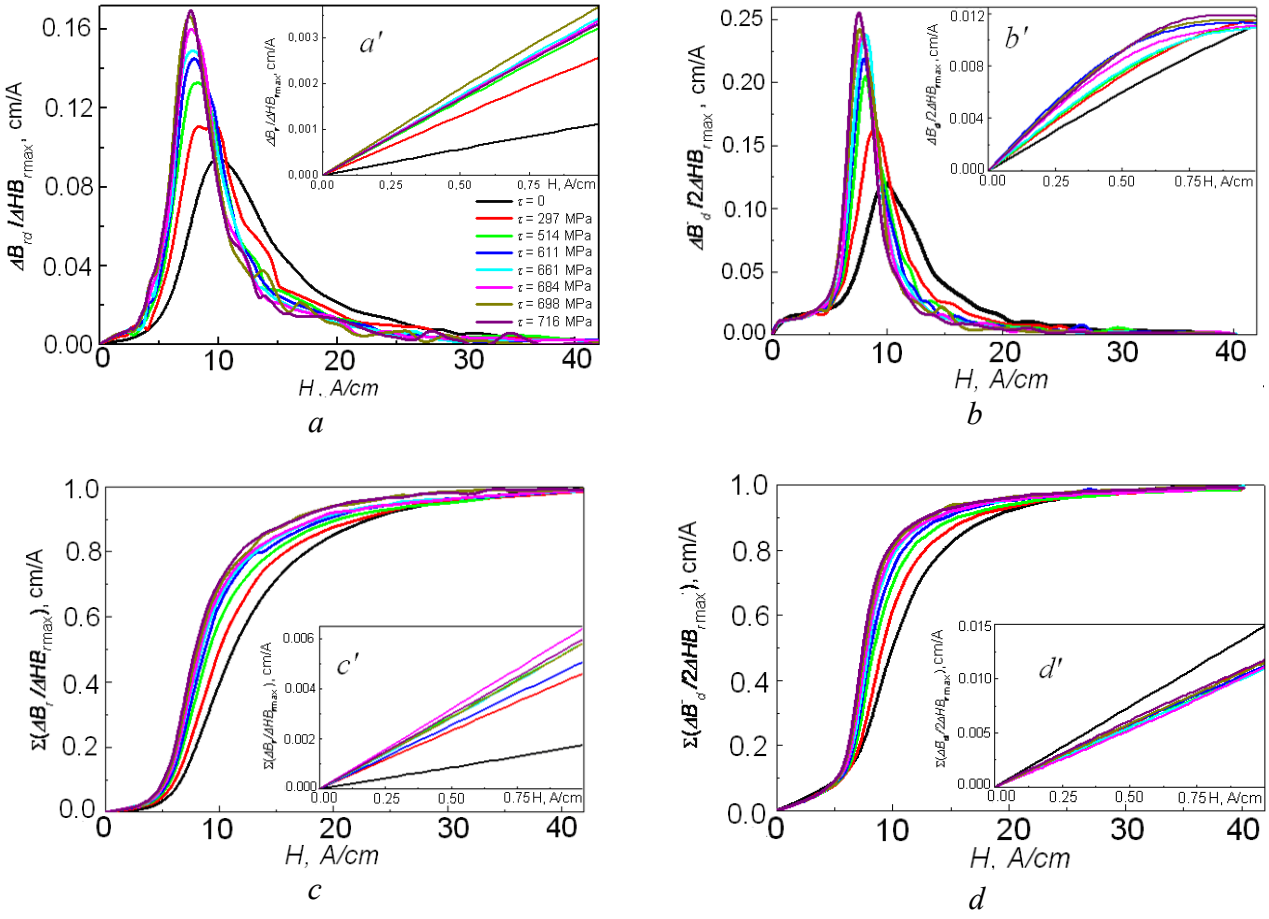

Fig. 5. The primary (*a*) and secondary (*b*) spectra of magnetic rigidity and the distributions of the volume fractions of critical fields under magnetization (*c*) and magnetization reversal (*d*) in torsion testing of steel 15CrNi4Cu. The initial portions of the rigidity spectra (*a', b'*) and the distributions of the critical field volumes (*c', d'*).

In tension and torsion, the curves of the field dependences of the quantities $\frac{\Delta B_r}{\Delta H \cdot B_{r\max}}$ (primary spectra) in the Rayleigh region, the same way as in compression, lie higher than without stresses, whereas the curves $\frac{\Delta B_d^-}{2\Delta H \cdot B_{r\max}}$ (secondary spectra) lie lower than in the unloaded state. That is, under the effect of tensile and torsional stresses, the stability of magnetic states under magnetization in the Rayleigh region from the demagnetized state is much lower than under magnetization reversal from the remanence state.

Thus, the processes of magnetization and magnetization reversal of steel 15CrNi4Cu affected by tensile, compressive or torsional stresses in the Rayleigh region obey to regularities different from those in the instance of the application of stronger magnetic fields. This manifests itself in the behaviour of the coercive force measured on the major and minor cycles of magnetic hysteresis, and

the distribution of critical fields in weak and strong magnetic fields. This must be taken into account when predicting changes in the magnetic state of products made of steel 15CrNi4Cu under the effect of normal and tangential stresses.

Conclusion

The coercive force of steel 15CrNi4Cu measured on the major hysteresis loop and on the minor cycle of magnetization reversal with the maximum induction of 0.4 T grows with elastic compressive stresses and decreases as normal tensile and shearing stresses grow. On the contrary, remanent induction and maximum magnetic permeability decrease as uniaxial elastic compressive stresses grow and increase as tensile stresses grow. This results from the positive magnetoelastic effect. Tangential stresses have little effect on remanent induction. After elastic stresses are relieved, the magnetic characteristics regain their initial values.

The coercive force measured on the minor cycles of magnetic magnetization reversal in weak fields grows linearly with normal elastic stresses. Apparently, the magnetization reversal and, consequently, magnetic hysteresis in weak fields are mainly due the displacement of 180° domain walls, that is why there are no signs of a magnetoelastic effect.

The uniqueness of the normal and shearing elastic stress dependences of the coercive force and the maximum magnetic permeability enables one to use these characteristics as parameters to evaluate compressive, tensile and torsional stresses. When predicting changes in the magnetic state of products made of steel 15CrNi4Cu occurring under the effect of normal and tangential stresses, it is essential to take into consideration that the processes of magnetization and magnetization reversal in this steel in the Rayleigh region and in the instance of stronger applied magnetic fields obey different laws.

The distributions of critical magnetic fields have been determined, and this offers information on the volume of a ferromagnet that has changed its state in a magnetic field of a given strength at certain mechanical stresses.

The study was partially supported by the RFBR (grant no 09-08-01091-a), the RAS Presidium (project “Fundamental problems of interaction mechanics in engineering and natural systems”) and the RAS Department of Power Engineering, Mechanical Engineering, Mechanics and Control Processes (project “Tribological and strength properties of structured materials and surface layers”).

REFERENCES

1. Vonsovsky S. V., Shur Ya. S. Ferromagnetism. M.-L.: OGIZ. 1948. 816 p.
2. Babich V. K., Pirogov V. A. On the nature of the variation of the coercive force in annealed carbon steels under deformation // FMM. 1969. V. 28. No 3. P. 447 – 453.
3. Atherton D. L., Jiles D. C. Effects of stress on magnetization // NDT International. 1986. V. 19. № 1. P. 15 – 19.
4. Makar J. M., Tanner B. K. The in situ measurement of the effect of plastic deformation on the magnetic properties of steel. Part I. Hysteresis loops and magnetostriction // J. Magn. Magn. Mater. 1998. V. 184. P. 193 – 208.
5. Gorkunov E. S., Zadvorkin S. M., Smirnov S. V., Mitropolskaya S. Yu., Vichuzhanin D. I. The relation of the parameters of the stress-strain state and the magnetic characteristics of carbon steels // FMM. 2007. 103. No 3. P. 322 – 327.
6. Gorkunov E. S., Zadvorkin S. M., Veselov I. N., Mitropolskaya S. Yu., Vichuzhanin D. I. The effect of uniaxial tension on the magnetic characteristics of pipe steel 12GB exposed to hydrogen sulphide // Defektoskopiya. 2008. No 8. P. 67 – 75.
7. Mikheev M. N., Gorkunov E. S. Magnetic methods of structural analysis and nondestructive testing. M.: Nauka, 1993. 252 p.
8. Deryagin A. V., Kandaurova G. S., Shur Ya. S. On the nature of magnetic rigidity in the plastically deformed Mn-Ga alloy // FMM. 1973. 35. No 2. P. 286 – 293.